Available online at website: https://journal.bcrec.id/index.php/bcrec

Bulletin of Chemical Reaction Engineering & Catalysis, 19 (3) 2024, 512-520

Research Article

Removal of Tetracycline Using Tungsten Disulfide/Graphene Oxide as Photocatalyst: Effect of Light Irradiation and Kinetic Studies

Zulhatiqah Zolekafeli[1], Syafarina Farisa Sateria[1], Ahmad Husaini Mohamed[1], Siti Hajar Alias[2], Kavirajaa Pandian Sambasevam[2,3], Siti Nor Atika Baharin[2*]

[1]School of Chemistry and Environment, Faculty of Applied Sciences, Universiti Teknologi MARA, Cawangan Negeri Sembilan, Kampus Kuala Pilah, 72000, Kuala Pilah, Negeri Sembilan, Malaysia.
[2]Advanced Materials for Environmental Remediation (AMER), Faculty of Applied Sciences, Universiti Teknologi MARA, Cawangan Negeri Sembilan, Kampus Kuala Pilah, 72000, Kuala Pilah, Negeri Sembilan, Malaysia.
[3]Electrochemical Material and Sensor (EMaS) Research Group, Universiti Teknologi MARA, Shah Alam, 40450 Selangor Malaysia.

Received: 17th August 2024; Revised: 21th September 2024; Accepted: 22th September2024
Available online: 16th October 2024; Published regularly: October 2024

Abstract

Once widely utilised in both human and veterinary medicine, tetracycline antibiotics are now recognised as major environmental pollutants with detrimental effects on the environment and human health. Concerns regarding allergic responses, gastrointestinal problems, and diseases resistant to antibiotics are raised by their persistence in soil, groundwater, and surface water. The production of a tungsten disulfide-graphene oxide nanocomposite for tetracycline degradation under varied light sources is presented in this work. The successful incorporation of tungsten disulfide on graphene oxide structures was confirmed by characterization using Attenuated Total Reflectance-Fourier Transform Infrared Spectroscopy (ATR-FTIR) and X-ray Diffraction (XRD). This revealed characteristic peaks for hydroxyl (3328 cm^{-1}), carbonyl (1732 cm^{-1}), alkene (1583 cm^{-1}), and ether (1044 cm^{-1}) bonds, as well as sulphur bonding (500 to 739 cm^{-1}). With a *D*-spacing of 2.24 nm, the tungsten disulphide-graphene oxide nanocomposite had a strong peak at $2\theta = 15.5^{\circ}$corresponds to the (002) plane, as shown by X-ray diffraction. A distinctive GO peak was found at $2\theta = 10.1^{\circ}$, which corresponds to the plane (002). With light emitting diodes (95.67%), fluorescent lights (81.28%), and ultraviolet-visible light (88.09%), the nanocomposite in a photoreactor showed excellent photocatalytic efficiency. The better performance of the tungsten disulfide-graphene oxide nanocomposite under varying illumination circumstances, as determined by the Langmuir-Hinshelwood (LH) model, presents a viable and sustainable option for tetracycline degradation in water purification. This technique tackles a long-term strategy for tetracycline photocatalytic degradation in water purification under different illumination scenarios.

Keywords: Photocatalysis; nanocomposite; tetracycline; graphene oxide; tungsten disulfide; kinetic study

How to Cite: Z. Zolekafeli, S.F. Sateria, S.H. Alias, K.P. Sambasevam, S.N.A. Baharin (2024). Removal of Tetracycline Using Tungsten Disulfide/Graphene Oxide as Photocatalyst: Effect of Light Irradiation and Kinetic Studies. *Bulletin of Chemical Reaction Engineering & Catalysis*, 19 (3), 512-520 (doi: 10.9767/bcrec.20204)

Permalink/DOI: https://doi.org/10.9767/bcrec.20204

1. Introduction

Pharmaceuticals are often employed in healthcare to maintain the health of both humans and animals, but this has unintentionally resulted in their accumulation in the environment, posing serious threats to both health and the environment [1]. Entire classes of pharmaceuticals, including hormones, antibiotics, painkillers, and many more prescription and over-the-counter drugs, can enter the environment through a number of pathways, including improper disposal, agricultural runoff, industrial discharge, and excretion from animals and humans After they are in the ecosystem, they could persist and have the potential to

* Corresponding Author.
Email: atikabaharin@uitm.edu.my (S.N.A. Baharin)

contaminate water supplies, disrupt ecosystems, and harm species [2,3]. The presence of pharmaceuticals in soil, natural water bodies, and even the air serves as a stark reminder of the unintended consequences of drug use. This highlights how important it is to grasp how medications affect the environment thoroughly.

When it comes to treating a wide range of bacteria, including Gram-positive and Gram-negative ones, tetracyclines (TC) antibiotic count among the drugs that are often employed in both veterinary and human healthcare [4]. Moreover, their broad-spectrum antibacterial properties are used to treat a variety of bacterial diseases, such as gonorrhoea and chlamydia, facial acne, infections of the respiratory system, urinary tract infections, and skin infections TC also have a great method of action that includes stopping bacteria from producing proteins where it inhibits the aminoacyl-tRNA from binding with the RNA-ribosome complex by adhering to the bacterial ribosome [5-7]. This process ultimately prevents the amino acids from being integrated into the growing peptide chain, which inhibits the growth and multiplication of bacteria.

Due to their extensive usage has severely damaged the environment, residual pollutants have frequently been discovered in soil, groundwater, and surface water. TC are very difficult for natural microbial processes to break down due to their low biodegradability and strong tendency to adhere to soil and sediment particles [8-9]. In addition, by having a complex molecular structure and chemical stability, TC can be challenging to break down in an environmentally friendly way. These characteristics extend the TC's resistance to chemical and biological degradation in the environment. Luckily, a variety of approaches nowadays might be investigated to promote TC breakdown while minimizing adverse environmental consequences. Green nanotechnology and advanced oxidation processes (AOPs) are two such potentially eco-friendly methods for TC breakdown [10-11]. By using ozonation and photocatalysis, for instance, AOPs degrade organic pollutants like TC by generating highly reactive hydroxyl radicals (˙OH) [12]. The use of nanostructured materials, such as metal nanoparticles or carbon-derived nanomaterials, as catalysts for the degradation of TC is also referred to as "green nanotechnology". Green synthesis strategies that employ plant materials or biocompatible polymers can be preferred over alternative methods to produce nanoparticles with a minimal environmental effect.

Therefore, through this experiment, tungsten disulfide (WS_2) and graphene oxide (GO) composites are considered as an effective catalyst in degrading TC among others due to their unique synergistic properties [13]. Owing to its two-dimensional structure, GO is noted to provide a high surface area which increases the number of active sites available for catalytic reactions when combined with WS_2. Moreover, GO has an excellent electrical conductivity which facilitating rapid electron transfer beneficial for catalytic processes involving electron transfer reactions [14]. Next, WS_2 are chosen to combine with GO to help in enhanced stability and durability for the composite because WS_2 is known for its chemical stability and resistance to harsh conditions which making it suitable for a long-term catalytic application [15-16].

Nevertheless, synergistic effects are formed when WS_2 and GO are combined where the characteristics of each part improve and complement the total catalytic activity [17]. For example, GO enhances dispersion and inhibits agglomeration of WS_2 particles, whereas WS_2 supplies active sites for catalysis. By varying the ratio of WS_2 to GO and the synthesis process, the characteristics of WS_2/GO composites may be customised, enabling the composite to be optimised for certain catalytic applications [18-19]. Due to the special combination of WS_2 and GO, the composite material can display multifunctional features, such as simultaneous electrocatalysis and photocatalysis, making WS_2/GO composites adaptable for a variety of catalytic processes. Additionally, the different oxygen functional groups found in GO have the ability to create defects into the WS_2 structure, resulting in the creation of extra active sites for catalysis and an increase in the composite material's catalytic activity. Hence in this study, by utilising the advantages of both materials, WS_2 and GO work together to create a composite catalyst that performs better overall in terms of activity, stability, and adaptability when degrading TC.

2. Materials and Methods

LabChem Sdn Bhd, a Malaysian company, provided the graphite powder required to make graphene. The following supplies were utilized, as supplied by LabChem Sdn Bhd, Malaysia: potassium permanganate ($KMnO_4$, 99%), sodium nitrate ($NaNO_3$, R&M Malaysia), concentrated hydrochloric acid (HCl, 37%, R&M brand, Malaysia), acetone, and methanol. The tetracycline came from Sigma Aldrich, located in Malaysia. NaH_2PO_4 and laboratory grade acetonitrile were supplied by the Malaysian business Merck Sdn Bhd. During the whole experiment, deionized water was used.

2.1 Synthesis of Tungsten Disulphide (Hydrothermal Method)

WS_2 was produced hydrothermally in an acidic atmosphere with tungstic acid and thiourea as the starting components. Generally, 1.5 g of tungstic acid and 1.9 g of thiourea were dissolved in 20 mL of deionized water and sonicated for 30 min. Subsequently, 1 M HCl solution was added to the mixture and stirred for an additional 30 min to bring the pH of the mixture to 2.0. After being hydrothermally treated for 24 h at 80 ˚C, the reaction mixture was moved to a 50 mL stainless-steel autoclave walled with Teflon and given time to cool to room temperature. After being repeatedly washed with ethanol and deionized water, the final product was centrifuged for 10 min at 4000 rpm. It was then dried for 12 h at 60 °C in a vacuum oven. The completed object was then kept in a desiccator for storage.

2.2. Synthesis of Graphene Oxide (GO) (Modified Hummer's Method)

Hummer's approach was adapted to create graphene oxide (GO). A standard procedure involved adding 1 g of graphite flakes, 0.5 g of sodium nitrate ($NaNO_3$) and 23 mL of concentrated sulfuric acid (H_2SO_4) to a 250 mL three-necked round-bottom flask. The flasks were then agitated for 1 h at ambient temperature and placed in an ice bath (0-5 °C). Next, gently add 3 g of potassium permanganate ($KMnO_4$) and mix vigorously for 1 h. Following the removal of the ice bath, the solution was stirred for a further 4 h. Following a half-hour of stirring, a water bath was used to get the temperature up to 35 °C. Subsequently, the suspension was heated to 70 ˚C after 250 millilitres of deionized water were added to the suspension. The final mixture was then whisked for 15 min. After the unreacted compounds were removed, a 30% hydrogen peroxide solution was added. By centrifuging and repeatedly washing with a 5% HCI solution, the GO was extracted. Lastly, a vacuum oven set at 70 °C was used to dry the slurry for the whole night.

Using an Ultraviolet-Visible Spectrometer (UV-Vis) between 200 and 900 nm, the concentration of tetracycline in the aqueous phase was determined. Tetracycline was broken down under various light source irradiation conditions, such as LED, fluorescent lamp, UV lamp, and total darkness, to evaluate the photocatalytic activity of tungsten disulphide/graphene oxide (WS_2/GO). The photoreactor utilized for the photocatalytic tests had four quartz tube reactors. In a typical photocatalytic experiment, 0.002 g of WS_2/GO composites were placed in a beaker and 20 mL of a stock solution containing 20 mg/L was added. To ensure that the adsorption/desorption equilibrium is attained, 0 mL and 50 mg/L (C_o) of each solution were then pipetted out and put in a UV photoreactor at the starting point ($t = 0$) for 30 min in a dark environment with steady stirring. Lastly, a UV-Vis spectrometer was used to detect the absorbance of solution samples in order to monitor the concentration of tetracycline during the photocatalytic decomposition process. The C/C_o ratio, where C is the tetracycline concentration at a certain time and C_o is the tetracycline concentration at t = 0 min was computed using the observed tetracycline absorption for each sample.

2.3. Synthesis of WS_2/GO

For 10 min, 40 mg of GO were ultrasonically dissolved in 40 mL of deionized water in a beaker. Next, 40 milliliters of deionized water were mixed with six milligrams of WS_2. The solution was then ultrasonically sonicated for 10 min. The precursor was finally centrifuged, rinsed with water, and dried in an 80 °C vacuum oven for 24 h. The synthesized composite, designated as WS_2/GO, is stored in a desiccator.

2.4. Instrumentation

Using the Fourier transform infrared (FTIR) method of attenuated total reflectance (ATR) (Spectrum 100 FTIR Spectrometer, Perkin Elmer) in the 4000–650 cm^{-1} range, the photocatalyst tungsten disulphide/graphene oxide composite is characterized continuously during this degrading process. An PG Instrument Ltd. T80 + UV/VIS Spectrometer was then used to measure the UV-Vis absorbance in the range of 200 to 900 nm. A Cu target was used in an Empyrean x-ray diffractometer operating at 40 kV and 40 mA to acquire an X-ray diffractogram (XRD) in the 2 theta (θ) with a range of 5-70˚.

2.5. Procedure

Using an Ultraviolet-Visible Spectrometer (UV-Vis) between 200 and 900 nm, the concentration of tetracycline in the aqueous phase was determined. Tetracycline was broken down under various light source irradiation conditions, such as LED, fluorescent lamp, UV lamp, and total darkness, to evaluate the photocatalytic activity of tungsten disulphide/graphene oxide (WS_2/GO). The photoreactor utilized for the photocatalytic tests had four quartz tube reactors. In a typical photocatalytic experiment, 0.002 g of WS_2/GO composites were placed in a beaker and 20 mL of 20 mg/L of TC was added. To ensure that the adsorption/desorption equilibrium is attained, 0 mL and 50 mg/L (C_o) of each solution were then pipetted out and put in a UV photoreactor at the starting point (t = 0) for 30 min in a dark environment with steady stirring. Lastly, a UV-Vis spectrometer was used to detect the absorbance of solution samples to monitor the

concentration of tetracycline during the photocatalytic decomposition process. The C/C_o ratio, where C is the tetracycline concentration at a certain time and C_o is the tetracycline concentration at $t = 0$ min was computed using the observed tetracycline absorption for each sample.

3. Results and Discussion

3.1. FTIR Analysis

The FTIR spectrums for GO, WS_2, and WS_2/GO are shown in Figure 1. The O-H stretching vibrations are responsible for the large peak centred at 3328 cm^{-1} in the FTIR spectra of GO. In the meanwhile, carbonyl (C=O), the C=C stretching mode, and C–O stretching are shown by absorption bands at 1732 cm^{-1}, 1583 cm^{-1}, and 1044 cm^{-1}, respectively. Subsequently, the WS_2 spectrum in Figure 1(b) displays numerous peaks at 657 cm^{-1} and 739 cm^{-1}, which are caused by the in-plane sulfur bonding (S-S) [13]. Similar spectrum range was obtained in synthesizing WS_2 [20], indicating that the method was properly conducted. In the meanwhile, the WS_2/GO spectrum shown in Figure 1(c) shows all the peaks observed in GO and WS_2 combined into a composite. This demonstrated the effective synthesis of the composite.

3.2. XRD Analysis

Figure 2 displays the XRD peaks of the GO, WS_2, and WS_2/GO composites. The large peak in the XRD pattern suggests that GO is amorphous. On the other hand, WS_2 has a crystalline structure with distinct peaks at $2\theta = 14.3^\circ$, 15.5°, 23.8°, 28.5°, 37.2°, and 43.2°, which represent the (002), (002), (004), (100), and (103) planes, in that order. JCPDS Card 08-0237 indicates that these peaks can be attributed to the hexagonal phase of WS_2 [15,18]. The (002) plane of WS_2 has a D-spacing of 2.24 nm, and the sharp peak at 15.5° corresponds to this plane. This suggests that layered WS_2 develops well along the c-axis throughout synthesis. This peak is also visible in the WS_2/GO nanocomposite's XRD pattern, indicating the creation of single-layer WS_2 in the sample. Furthermore, there is the distinctive GO peak at $2\theta = 10.1^\circ$, which is located in the (002) plane. Due to a larger ratio of GO to WS_2, the diffractogram of the composite shows that GO sheets predominate in the WS_2/GO hybrids, with the typical peaks of WS_2 being easily apparent [23,32].

Furthermore, the GO inclusion resulted in a 3.6 nm crystallite size in the WS_2/GO composites by decreasing their crystallinity. This decrease is explained by the full dispersion of GO in the composite. The Scherrer equation (Eq. 1) was utilized to compute the size of the crystallite [12].

$$D = \frac{0.9\,\lambda}{\beta \cos\theta} \quad (1)$$

where λ is the X-ray wavelength, β is the full width at half maximum (FWHM) of the X-ray diffraction peak in radians, D is the crystallite mean size (nm), k is the crystallite form factor (usually assumed as 0.9), and θ is the Bragg angle (degrees). Because WS_2 is crystalline, it has a high crystallinity size of 8.34 nm. According to the findings, bigger surface areas correlate with smaller crystallite sizes [23-24]. This phenomenon enhances the generation of radicals by facilitating the passage of light-induced carriers to the outermost particles.

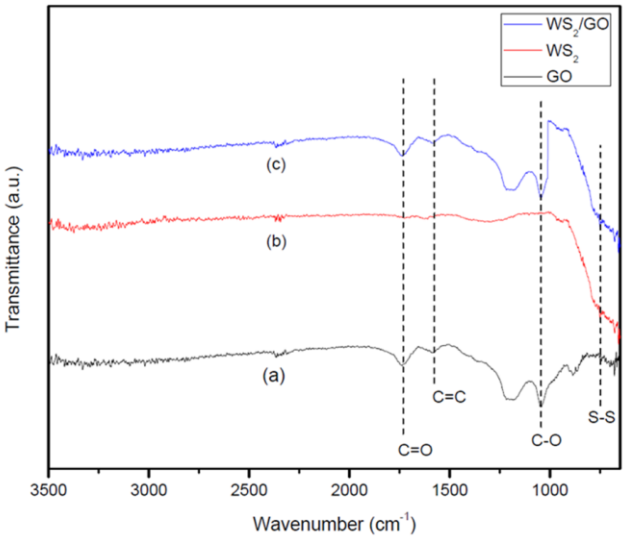

Figure 1. FTIR spectrum for (a) graphene oxide (GO), (b) tungsten disulphide (WS_2), and (c) tungsten disulphide- graphene oxide (WS_2/GO).

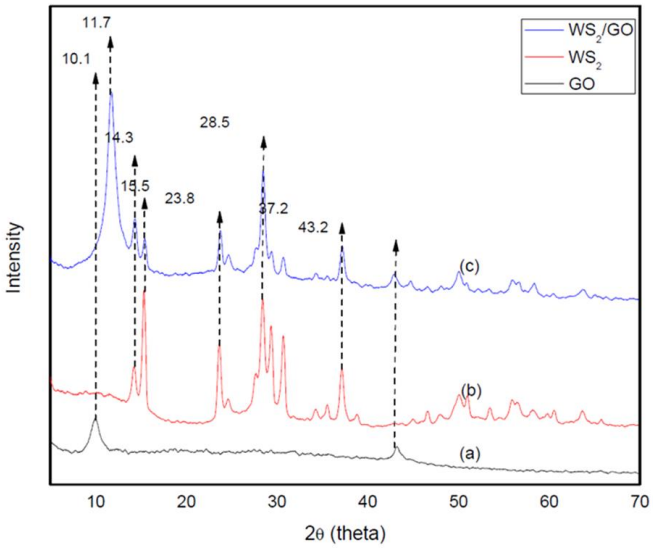

Figure 2. XRD spectrum of (a) GO, (b) WS_2, and (c) WS_2/GO composites.

3.3. Surface Area Analysis

Using nitrogen as the analysis gas, the Brunauer-Emmett-Teller analysis was performed to calculate the surface area of the photocatalysts WS_2 and WS_2/GO composites using adsorption and desorption isotherms. Prior to each measurement, 0.03 g of each powdered catalyst was weighed and degassed under vacuum for 12 h at 150 °C. After then, the catalysts were exposed to 1 h of 100 °C outgassing. The adsorption-desorption isotherms of nitrogen obtained for the WS_2 and WS_2/GO composites, were classified by BET as TYPE H4 [25] as shown in Figure 3. This type of isotherm forms a convex shape to the x-axis throughout its entire range, with the observation of hysteresis, a phenomenon typically observed in mesoporous structures (2 nm <size<50 nm) [26].

The physicochemical characteristics of GO, WS_2, and WS_2/GO are reported in Table 1. The range of GO's specific surface area was 2 to 1000 $m^2.g^{-1}$ [22]. As GO tends to cluster together when dried, the value received from the results is significantly lower than the predicted value. It's generally understanding that GO can be dispersed evenly and fully exfoliated. Based on available research, the specific surface area of WS_2 was determined to be between 5.00 and 20.00 $m^2.g^{-1}$ [27]. The combination of WS_2 and GO can significantly minimize the restacking of WS_2 layers and the graphene layer, as indicated by the results, which show that the specific surface area of WS_2/GO is larger than that of both GO and WS_2. The GO and WS_2 nanoparticles tend to aggregate, decreasing their surface area. However, the specific surface area rose following the intercalation of WS_2 and GO. An increase in surface area results in enhanced photocatalytic activity and an improved adsorption transport pathway. Furthermore, the WS_2/GO composites' decreased pore size after merging indicates that the pores between these materials are filled and integrated with one another.

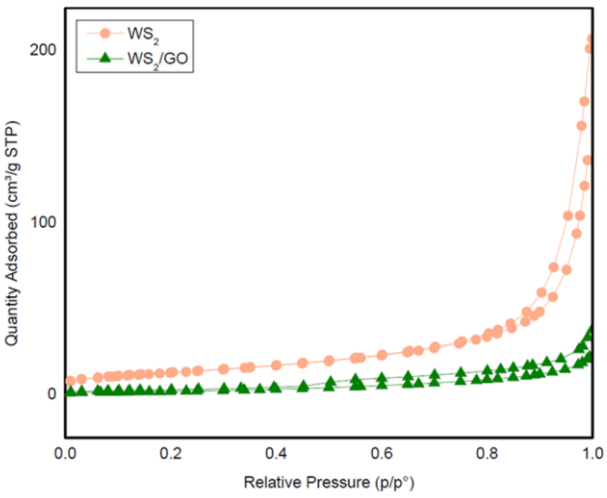

Figure 3. BET plot of nitrogen adsorption isotherm of WS_2 and WS_2/GO nanocomposite.

3.4. Photocatalytic Degradation Analysis

Water-soluble tetracycline antibiotic solution was used to photodegrade the virgin WS_2, GO, and WS_2/GO composites to evaluate their photocatalytic performance. The purpose of the light source effect study was to establish a connection between the characterisation analysis of composites and their capacity to break down the antibiotic tetracycline. This study assessed four distinct irradiation settings for 180 min: dark, LED, UV, and fluorescent. The degradation efficiency of TC by using GO, WS_2, and WS_2/GO nanocomposites as photocatalyst under the specified irradiations are shown in Figure 4. The figure revealed that all photocatalysts perform poorly at degradation under dark settings, with physisorption playing a major role in controlling degradation. In contrast, as shown in Figure 4 and Table 2, the degradation efficiency of WS_2/GO (95.67%) outperformed other photocatalysts-GO (82.41%) and WS_2 (84.31%) in terms of degrading performance when light emitting diodes (LEDs) were present. This is because there is enough WS_2, or visible active photocatalyst. Moreover, the separation efficiency of photogenerated electron pairs in WS_2/GO composites was significantly enhanced by the addition of GO. Notably, the surface-active sites of the photocatalyst were enhanced by the addition of GO [22].

3.5. Contact Time and Kinetic Analysis

The materials were evaluated for 30 min in the dark and then for 0 to 180 min under LED irradiation in order to further examine the impact of contact time on the kinetic behaviour of the photodegradation process. As Figure 5 illustrates, there was very little deterioration in the dark, and

Table 1. Brunauer-Emmett-Teller (BET) and Barrett-Joyner-Halenda (BJH) cumulative pore volume analysis of GO, WS_2, and WS_2/GO composites

	BET Analysis	BJH Analysis	
Materials	BET Surface Area ($m^2.g^{-1}$)	Pore size (nm)	Pore Volume (cm^3/g)
GO	2.509	15.6349	0.012167
WS_2	1.2119	6.02311	0.012219
WS_2/GO	7.8637	5.6977	0.001800

the variations suggested that an equilibrium between adsorption and desorption had been established. From 0 to 30 min, there was rapid decline; from 150 to 180 min, there was a progressive drop and final standstill. Tetracycline degraded quickly at first because the photocatalyst's active sites were still empty, enabling quick degradation. Tetracycline's rate of degradation was slowed down when more active sites were filled since this lessened the possibility of electron-hole recombination. Extensive studies on heterogeneous photocatalysts in organic pollutants photo-degradation have demonstrated that the result is consistent with the Langmuir-Hinshelwood (LH) kinetic model (Eq. 2):

$$r_0 = -\frac{dC}{dt} = \frac{kKC}{1+KC} \quad (2)$$

Table 2. Degradation percentage of GO, WS_2, and WS_2/GO under different conditions

Conditions	GO	WS_2	WS_2/GO
Dark	6.78	10.06	31.02
Fluorescent	64.61	70.8	81.28
UV	81.65	83.8	88.09
LED	82.41	84.31	95.67

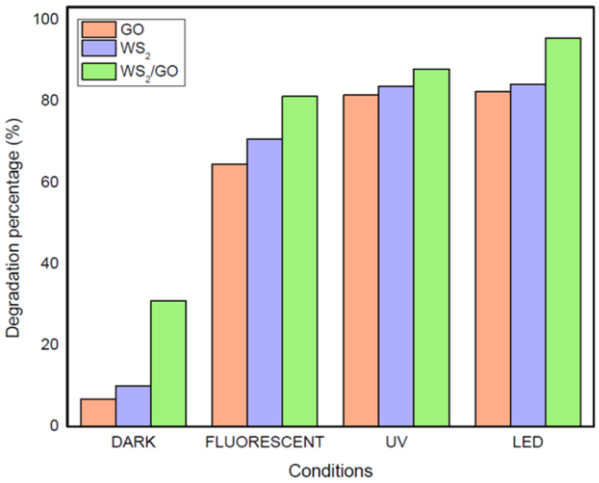

Figure 4. Degradation percentage of GO, WS_2, and WS_2/GO under different conditions.

where, K is the adsorption equilibrium constant, k is the reaction rate constant, r_o is the reactant's decomposition rate, and C is the concentration of the reactant. K_c « 1 in the LH equilibrium may be lowered to a pseudo-first-order kinetic model (Eq. 3) due to the low dose of tetracycline antibiotics utilized in the experiment:

$$-\frac{dC}{dt} = kKc = k_{obs}C \quad (3)$$

When the threshold of $C = G_o$ is further fixed at $t = 0$, it is possible to integrate Eq. 3, leading to (Eq. 4):

$$-ln\frac{C}{C_o} = k_{obs}t \quad (4)$$

Table 3 exhibit the kinetic constants for the observed values pseudo-first-order of this study along with different references regarding photocatalytic degradation of TC. Through this study, the rate constant k, coefficient of determination R^2, and half-life $t_{1/2}$ were found to be, respectively, 0.0797 min^{-1}, 0.9998, and 8.695 min^{-1}, based on a plot of ln C/C_o vs. irradiation

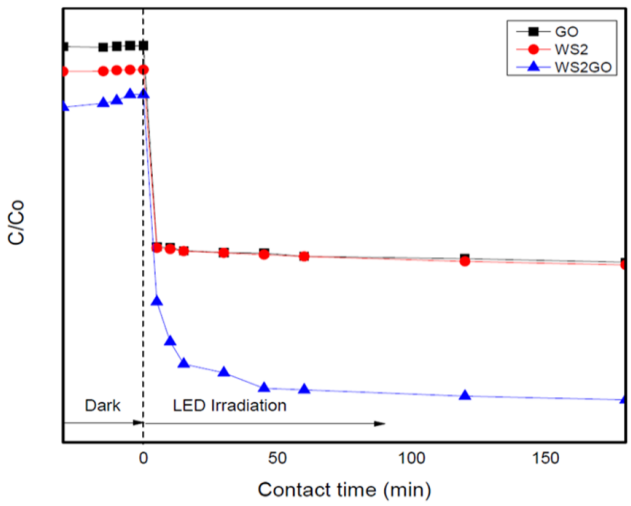

Figure 5. Effect of contact time for photocatalytic degradation of tetracycline antibiotic (20 mg/L tetracycline antibiotic, 12-watt light emitting diode irradiation, 0.002 g/L of catalyst loading).

Table 3. Pseudo-first order (kinetic parameters) of different types of photocatalyst and light sources in degrading tetracyclines.

Type of Photocatalyst	Light Source	Contact time (min)	Initial concentration (mg/L)	k (min^{-1})	$t_{1/2}$ (h)	Degradation (%)	Ref.
ZnO	UV	180	0.0016	Not mention	Not mention	93.3	[28]
TiO_2	UV	120	55	0.0163	42.5	83.2	[29]
B-TiO_2	Xenon lamp	240	10	0.0045	Not mention	66.2	[30]
MWCNT-TiO_2	UV	60	10	0.064	Not mention	92.2	[31]
WS_2/GO	LED	120	50	0.0797	0.1449	95.67	This study

length shown in Figure 6. Figure 7 illustrates schematic diagram the photogenerated electrons in the conduction band (CB) of WS_2 would migrate to GO while the holes in the valence band (VB) of WS_2 could transfer to GO. As a result, the recombination of formed electrons and holes could be prevented greatly.

4. Conclusions

To sum up, the hydrothermal approach and modified Hummer's method were successfully used to manufacture all three GO, WS_2, and WS_2/GO composites. These composites were then used as a catalyst for the photodegradation of tetracycline under various light irradiation conditions. The effective synthesis was demonstrated throughout the FTIR study, as the composites of WS_2/GO showed all of the peaks found in GO and WS_2 merged into a composite. Furthermore, throughout the XRD examination, WS_2/GO composites exhibit a 3.6 nm decrease in crystallite size following the addition of GO to WS_2. This combination increases the production of radicals during the tetracycline degradation process. Next, the WS_2/GO composite is classified as a TYPE 4 based on its hysteresis properties, with a convex shape parallel to the x-axis and a mesoporous size of 5.6977 nm. With all of the features demonstrated by the WS_2/GO composites, LED light sources displayed the highest tetracycline degradation of 95.67% among all light situations. As a result, tetracycline degradation was shown to be successful in the presence of LED light sources and WS_2/GO as catalyst.

Acknowledgment

We acknowledge the School of Chemistry and Environment, Faculty of Applied Science UiTM Negeri Sembilan, Kuala Pilah Campus for the facilities that were provided for the research. This project was supported by financial grants such as the Fundamental Research Grant Scheme [FRGS/1/2022/STG05/UITM/02/12] by Ministry of the Higher Education Malaysia. This research article was financially supported by Universiti Teknologi MARA and Institute of Postgraduate Studies UiTM.

CRediT Author Statement

Credit author statement: Zulhatiqah Zolekafeli: Investigation, Methodology, and original draft preparation. Syafarina Farisa Sateria: Investigation, Methodology. Siti Nor Atika Baharin: Visualization and supervision. Kavirajaa Pandian Sambasevam: Visualization and conception design of the study. Ahmad Husaini Mohamed: Visualization and supervision. Siti Hajar Alias: Writing – review & editing.

References

[1] Khetan, S.K., Collins, T.J. (2007). Human Pharmaceuticals in the Aquatic Environment: A Challenge to Green Chemistry. *Chemical Reviews*, 107(6), 2319–2364. DOI: 10.1021/cr020441w

[2] Sawant, S.A., Riyaz Patankar, U., Kasale, A.S., Tawade, S.S. (2015). Pharmaceutical Pollution: Impact On Environmental Sustainability and Management. *World Journal of Pharmaceutical Research*, 10. DOI: 10.20959/wjpr202111-21436

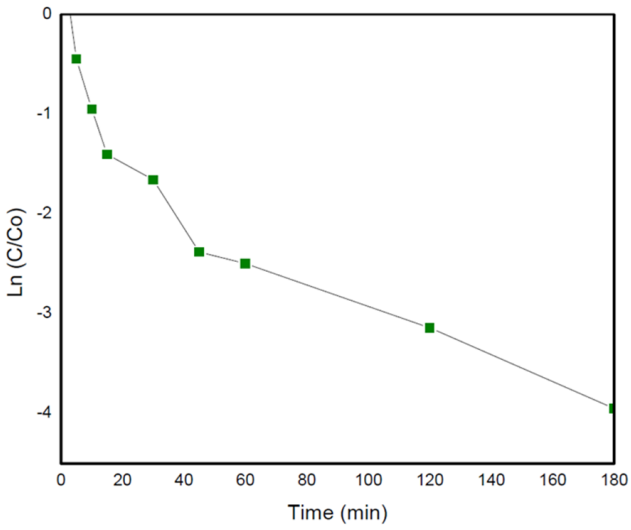

Figure 6. Kinetic plot of ln (C/C_0) versus irradiation time for the photocatalytic degradation of tetracycline antibiotics.

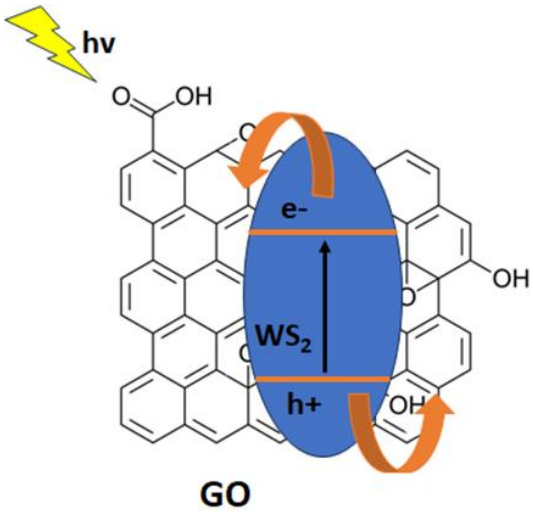

Figure 7. Schematic diagram of photogenerated electrons/hole in the WS_2/GO composites

[3] Dhawande, A., Moon, S., Kale, V., Pethe, A.M., & Raut, N.A. (2023). Pharmaceutical Waste: An Emerging Threat to The Ecosystem. *In 360-Degree Waste Management*, 2, 3–37. DOI: 10.1016/B978-0-323-90909-9.00008-3

[4] Daghrir, R., Drogui, P. (2013). Tetracycline Antibiotics in The Environment: A Review. *Environmental Chemistry Letters*, 11(3), 209–227. DOI: https://doi.org/10.1007/s10311-013-0404-8

[5] Adya, K.A., Inamadar, A.C. (2015). Comprehensive Approach to Infections in Dermatology (Archana Singal & Chander Grover, Eds.; Illustrated). JP Medical Ltd, 2016.

[6] Goodman C.C., Peterson, C., Komp, M. (2011). Pathology for the Physical Therapist Assistant (Catherine Cavallaro Kellogg & Kenda S. Fuller, Eds.; Revised, p. 128). Elsevier Health Sciences, 2011.

[7] Chopra, I., Roberts, M. (2001). Tetracycline Antibiotics: Mode of Action, Applications, Molecular Biology, and Epidemiology of Bacterial Resistance. *Microbiology and Molecular Biology Reviews*, 65(2), 232–260. DOI: 10.1128/MMBR.65.2.232-260.2001

[8] Mora-Gamboa, M.P.C., Rincón-Gamboa, S.M., Ardila-Leal, L.D., Poutou-Piñales, R.A., Pedroza-Rodríguez, A.M., Quevedo-Hidalgo, B.E. (2022). Impact of Antibiotics as Waste, Physical, Chemical, and Enzymatical Degradation: Use of Laccases. *Molecules,* 27(14), 4436. DOI: 10.3390/molecules27144436

[9] Bhattacharyya, P., Basak, S., Chakrabarti, S. (2021). Advancement Towards Antibiotic Remediation: Heterostructure and Composite Materials. *ChemistrySelect*, 6(29), 7323-7345. DOI: 10.1002/slct.202100436

[10] Gopal, G., Alex, S.A., Chandrasekaran, N., Mukherjee, A. (2020). A Review On Tetracycline Removal From Aqueous Systems By Advanced Treatment Techniques. *RSC Advances*, 10(45), 27081–27095. DOI: 10.1039/D0RA04264A

[11] Ahmad, F., Zhu, D., Sun, J. (2021). Environmental Fate of Tetracycline Antibiotics: Degradation Pathway Mechanisms, Challenges, and Perspectives. *Environmental Sciences Europe*, 33(1), 64. DOI: 10.1186/s12302-021-00505-y

[12] Hassani, A., Krishnan, S., Scaria, J., Eghbali, P., Nidheesh, P.V. (2021). Z-Scheme Photocatalysts for Visible-Light-Driven Pollutants Degradation: A Review on Recent Advancements. *Current Opinion in Solid State and Materials Science*, 25(5), 100941. DOI: 10.1016/j.cossms.2021.100941

[13] Zhang, W., Lv, T., Deng, C., Gao, H., Hu, S., Chen, F., ... Xiong, W. (2022). Rapid Solid-Phase Sulfurization Growth and Nonlinear Optical Characterization of Transfer-Free TiS_3 Nanoribbons. *Chemistry of Materials*, 34(6), 2790-2797. DOI: 10.1021/acs.chemmater.2c00068

[14] Fiaz, M., Sohail, M., Nafady, A., Will, G., Wahab, M.A. (2023). A Facile Two-Step Hydrothermal Preparation of 2D/2D Heterostructure of Bi_2WO_6/WS_2 For the Efficient Photodegradation of Methylene Blue Under Sunlight. *Environmental Research*, 234, 116550. DOI: 10.1016/j.envres.2023.116550

[15] Lei, T., Chen, W., Huang, J., Yan, C., Sun, H., Wang, C., Xiong, J. (2017). Multi-Functional Layered WS2 Nanosheets for Enhancing The Performance of Lithium–sulfur Batteries. *Advanced Energy Materials*, 7(4), 1601843. DOI: 10.1002/aenm.201601843.

[16] Amangelsin, Y., Semenova, Y., Dadar, M., Aljofan, M., Bjørklund, G. (2023). The Impact of Tetracycline Pollution on The Aquatic Environment and Removal Strategies. *Antibiotics*, 12(3), 440. DOI: 10.3390/antibiotics12030440

[17] Navalon, S., Dhakshinamoorthy, A., Alvaro, M., Garcia, H. (2016). Metal Nanoparticles Supported on Two-Dimensional Graphenes as Heterogeneous Catalysts. *Coordination Chemistry Reviews,* 312, 99–148. DOI: 10.1016/j.ccr.2015.12.005

[18] Muniz, F.T.L., Miranda, M.A.R., Morilla dos Santos, C., Sasaki, J.M. (2016). The Scherrer Equation and The Dynamical Theory of X-Ray Diffraction. *Acta Crystallographica Section A Foundations and Advances*, 72(3), 385–390. DOI: 10.1107/S205327331600365X

[19] Das, R., Laha, J., Hazarika, I., Thakuria, B.R., Baruah, A., Gogoi, B. (2024). Tungsten Disulfide and Reduced Graphene Oxide Composite as Efficient Catalyst for The Reduction of Picric Acid in Aqueous Media. *Journal of Materials Science*, 59(9), 3839–3857. DOI: 10.1007/s10853-024-09465-z

[20] Monshi, A., Foroughi, M.R., Monshi, M.R. (2012). Modified Scherrer Equation to Estimate More Accurately Nano-Crystallite Size Using XRD. *World Journal of Nano Science and Engineering*, 02(03), 154–160. DOI: 10.4236/wjnse.2012.23020

[21] Yang, Z., Ren, X., Ding, S., Chen, R., & Tian, M. (2023). Preparation of 1 T-WS_2 Under Different Conditions and Its Enhancement of Fe(III)/Fe (II) Cycle, Synergistic Catalysis of PMS Activation and Degradation of Organic Pollutants. *Journal of Environmental Chemical Engineering*, 11(6), 111444. DOI: 10.1016/j.jece.2023.111444

[22] Norsham, I.N.M., Sambasevam, K.P., Shahabuddin, S., Jawad, A.H., Baharin, S.N.A. (2022). Photocatalytic Degradation of Perfluorooctanoic Acid (PFOA) Via Mos_2/Rgo For Water Purification Using Indoor Fluorescent Irradiation. *Journal of Environmental Chemical Engineering*, 10(5), 108466. DOI: 10.1016/j.jece.2022.108466

[23] Zhou, L., Yan, S., Lin, Z., Shi, Y. (2016). In Situ Reduction of WS_2 Nanosheets for WS_2/Reduced Graphene Oxide Composite With Superior Li-Ion Storage. *Materials Chemistry and Physics*, 171, 16–21. DOI: 10.1016/j.matchemphys.2015.12.061

[24] Singh, O., Singh, M.P., Kohli, N., Singh, R.C. (2012). Effect of pH on The Morphology and Gas Sensing Properties of Zno Nanostructures. *Sensors and Actuators B: Chemical*, 166–167, 438–443. DOI: 10.1016/j.snb.2012.02.085

[25] Ambroz, F., Macdonald, T.J., Martis, V., Parkin, I. P. (2018). Evaluation of the BET Theory for the Characterization of Meso and Microporous MOFs. *Small Methods*, 2(11). DOI: 10.1002/smtd.201800173

[26] Nugraha, R.E., Fauziyah, N.A., Wira, G.R. (2022). Templated Growth Formation Of Mesoporous Silica Materials: A Soft-Hard Template Approach. *Nusantara Science and Technology Proceedings*. DOI: 10.11594/nstp.2022.2747

[27] Peng, K., Wang, H., Li, X., Wang, J., Cai, Z., Su, L., Fan, X. (2019). Emerging WS_2/Montmorillonite Composite Nanosheets As An Efficient Hydrophilic Photocatalyst For Aqueous Phase Reactions. *Scientific Reports*, 9(1), 16325. DOI: 10.1038/s41598-019-52191-9

[28] Wang, H., Yao, H., Pei, J., Liu, F., & Li, D. (2016). Photodegradation of Tetracycline Antibiotics in Aqueous Solution by UV/Zno. *Desalination and Water Treatment*, 57(42), 19981–19987. DOI: 10.1080/19443994.2015.1103309

[29] Safari, G.H., Hoseini, M., Seyedsalehi, M., Kamani, H., Jaafari, J., Mahvi, A.H. (2015). Photocatalytic Degradation of Tetracycline Using Nanosized Titanium Dioxide In Aqueous Solution. *International Journal of Environmental Science and Technology*, 12(2), 603–616. DOI: 10.1007/s13762-014-0706-9

[30] Wu, S., Li, X., Tian, Y., Lin, Y., Hu, Y.H. (2021). Excellent Photocatalytic Degradation of Tetracycline over Black Anatase-TiO_2 under Visible Light. *Chemical Engineering Journal,* 406, 126747. DOI: 10.1016/j.cej.2020.126747

[31] Ahmadi, M., Ramezani Motlagh, H., Jaafarzadeh, N., Mostoufi, A., Saeedi, R., Barzegar, G., Jorfi, S. (2017). Enhanced Photocatalytic Degradation of Tetracycline and Real Pharmaceutical Wastewater using MWCNT/TiO_2 Nano-Composite. *Journal of Environmental Management*, 186, 55–63. DOI: 10.1016/j.jenvman.2016.09.088

[32] Khataee, A., Eghbali, P., Irani-Nezhad, M.H., Hassani, A. (2018). Sonochemical Synthesis Of WS_2 Nanosheets and Its Application in Sonocatalytic Removal of Organic Dyes from Water Solution. *Ultrasonics Sonochemistry*, 48, 329–339. DOI: 10.1016/j.ultsonch.2018.06.003